

A new yttrium-rich garnet species, $\{(Y,REE)(Ca,Fe^{2+})_2\}[(Mg,Fe^{2+})(Fe^{3+},Al)](Si_3)O_{12}$: Implications for the prograde metamorphic path in the Parry Sound domain, Central Gneiss Belt, Grenville Orogenic Province

Edward S. Grew*, Jeffrey H. Marsh, and Martin G. Yates
 Department of Earth Sciences, University of Maine, Orono, Maine 04469-5790, USA
 esgrew@maine.edu

Summary

A new garnet species containing up to 28 wt % $(Y,REE)_2O_3$ (1.1 Y,REE per 12 O) occurs in a granulite consisting dominantly of oligoclase, quartz, and ferrosilite; augite, calcic amphibole, biotite, almandine, ilmenite, magnetite, apatite-(CaF), allanite-(Ce), zircon, monazite-(Ce), xenotime-(Y) are subordinate to sparse constituents. We infer that the new Y-rich garnet is an early mineral formed at $P \sim 7$ -8.5 kbar and $T \sim 700$ -800°C, and that armoring by almandine and K-feldspar subsequently preserved it. There is no microstructural evidence for almandine being present when the Y-rich garnet was stable. Breakdown of the Y-rich garnet is associated with partial melting, when it dissolved incongruently in the melt to give peritectic almandine at $P \sim 8.5$ -9.5 kbar and $T \sim 800$ -850°C. A possible source of Y and heavy REE for the Y-rich garnet could have been xenotime-(Y). Had almandine been present, it would have incorporated the Y and HREE released by breakdown of xenotime-(Y), and Y-rich garnet would not have formed.

Introduction

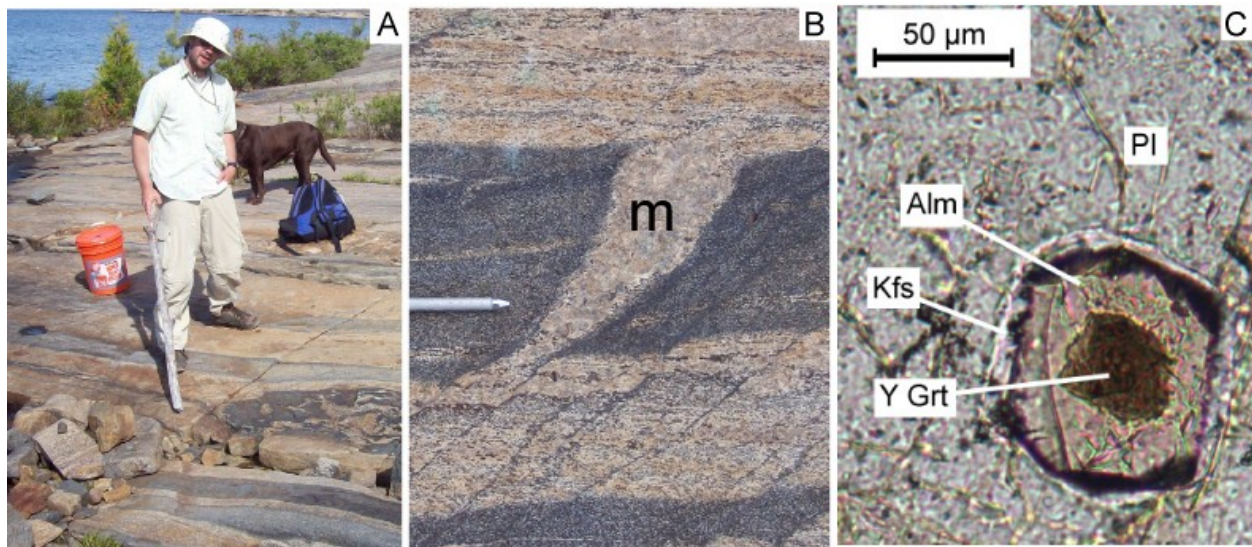


Figure 1A and B: Type locality on Bonnet Island. A. Jeffrey Marsh is pointing to the layer containing the new Y-rich garnet. B. Melt filling neck in boudinaged mafic granulite in the layered sequence. C. Photomicrograph of the new Y-rich garnet enclosed in almandine surrounded by K-feldspar in a plagioclase matrix. Plane-polarized light

The yttrium contents of common metamorphic and plutonic garnets typically range from several hundred ppm to several thousand ppm, but in a few pegmatitic garnets, up to 24800-26500 ppm (3.15-3.36 wt% Y_2O_3) are present (Enami et al. 1995; Kasowski and Hogarth 1968), corresponding to 0.14-0.15 Y per formula unit (p.f.u.) of 8 cations and 12 oxygen atoms. We

found a garnet containing ≤ 17 wt% Y_2O_3 and ≤ 12 wt % $(REE)_2O_3$ (maximum 1.1 Y,REE p.f.u.) as an accessory mineral in euhedral almandine in a pyroxene-plagioclase granulite (Fig. 1c) on Bonnet Island (UTM coordinates 0567531W 5003719N; NAD 83 datum), an exposure of well-layered granulite-facies supracrustal rocks (Fig. 1a, b) in the interior Parry Sound Domain (iPSD), Central Gneiss Belt, Grenville Province, and part of an allochthonous terrane near the highest structural level of a thrust stack assembled at ~ 1120 -1090 Ma (Davidson et al., 1982; Culshaw et al., 1997). This Y-rich garnet is a new mineral (end member $Y_2CaMg_2Si_3O_{12}$) approved by the Commission on New Minerals, Nomenclature and Classification, International Mineralogical Association (IMA 2009-050, Grew et al., in preparation).

Our objective in the present abstract is to show how reactions involved in the growth and dissolution of the Y-rich garnet fit into the prograde history of the iPSD rocks.

Analytical Methods

Minerals were analyzed with a Cameca SX-100 electron microprobe using wavelength dispersive spectroscopy at U Maine. Special protocols with two-column conditions were developed for the new Y-rich garnet, allanite-(Ce), monazite-(Ce) and apatite-(CaF); silicates containing little Y+REE were analyzed under standard conditions (Grew et al., in preparation).

Microstructures

The granulite containing the new garnet (Fig. 1a) consists dominantly of oligoclase (An₂₅₋₂₈), quartz, and ferrosilite ($Fs_{56-61}En_{38-43}Wo_{1-3}$ plus $\sim 1\%$ MnSiO₃); augite ($Fs_{27-29}En_{29-30}Wo_{41-43}$), calcic amphibole, biotite, almandine, ilmenite and magnetite are subordinate. Accessories include widespread apatite-(CaF), allanite-(Ce), and zircon, plus sparse monazite-(Ce), xenotime-(Y), sulfides, and hercynite.

Evidence for intense deformation includes preferred orientation due to flattening of ferrosilite aggregates and individual ferrosilite and plagioclase grains and bending of plagioclase twin lamellae. Larger plagioclase grains (mostly 1-3 mm long) are surrounded by much finer-grained recrystallized plagioclase.

Grains of the Y-rich garnet, up to 75 μ m, commonly have irregular borders, and, locally, atoll-like microstructures (Fig. 2a). The new garnet is for the most part isolated from the other phases by almandine or K-feldspar and no contacts with oligoclase, quartz, or ferrosilite were found.

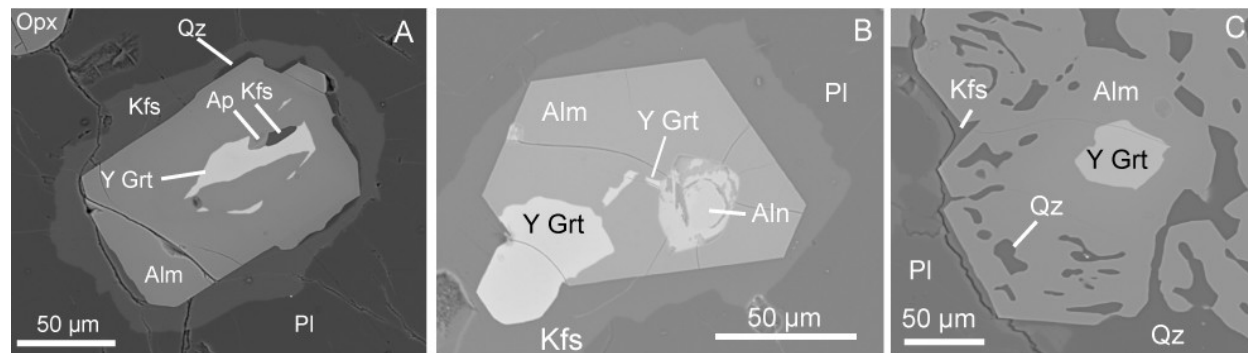


Figure 2: Backscattered electron images of the new Y-rich garnet enclosed in almandine with apatite-(CaF), allanite-(Ce), K-feldspar and quartz.

Almandine surrounding the Y-rich garnet is euhedral, in places, with remarkably smooth faces and sharp corners (Fig. 2b), and is surrounded by moats of K-feldspar, locally with quartz (Fig. 2a). In some cases, almandine overgrowing inclusion-poor almandine around the new garnet contains quartz vermicules (Fig. 2c). Symplectite containing augite as well as quartz (Fig. 3a) is common around ferrosilite, magnetite and ilmenite (Fig. 3c). One sample contains a distinctive symplectite of almandine, quartz and biotite, the last forming decussate aggregates (Fig. 3b).

Ferrosilite grains 1 to 3 mm long range from elongate to subequant; borders are commonly highly irregular with pointy extensions. Augite occurs also as independent grains up to 5 mm long. Calcic amphibole grains are irregular and on average finer (0.2-1 mm long) than pyroxene; and typically overgrow pyroxene or Fe-Ti oxide. K-feldspar is a minor constituent; its most distinctive microstructures are moats around quartz (Fig. 3c) and almandine (Fig. 2), but antiperthitic lamellae in oligoclase and irregular masses up to 0.5 mm are also found.

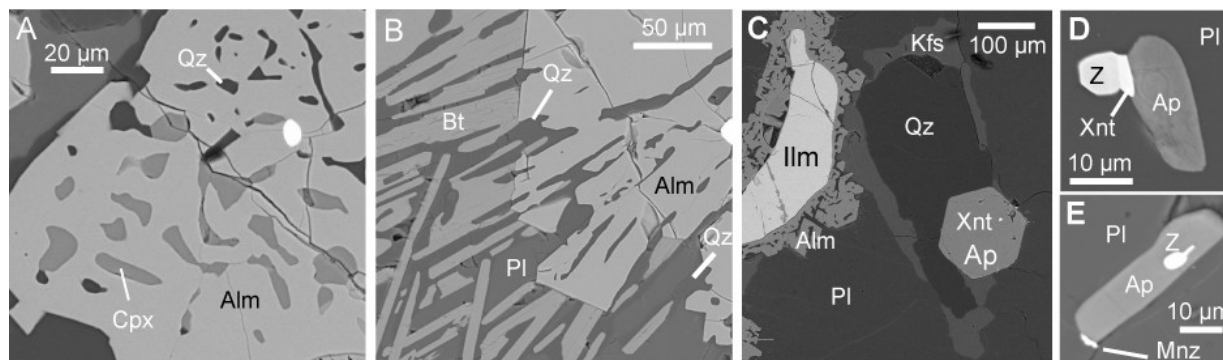


Figure 3: Backscattered electron images of almandine-augite-quartz symplectite, almandine-biotite-quartz symplectite, K-feldspar moat around quartz, xenotime-(Y) and monazite-(Ce) with apatite-(CaF). Z – zircon.

Allanite-(Ce) is the most widespread of the four REE phases, occurring as highly zoned and partially altered grains from 0.1 to 0.45 mm long and rarely in almandine (Fig. 2b). Xenotime-(Y) and monazite-(Ce) have been found as very rare inclusions in apatite-(CaF) (Fig. 3c) or contiguous to it (Fig. 3d, e).

Phase Relations and Pressure-Temperature Evolution

We infer from the microstructures that the new Y-rich garnet is an early-formed mineral originally in contact with plagioclase, quartz, ferrosilite, magnetite, ilmenite and possibly augite and that being armored by almandine and K-feldspar subsequently preserved it. There is no microstructural evidence for almandine being present when the Y-rich garnet was stable. This absence is surprising given the relatively high bulk-rock atomic $Fe^{2+}/(Fe+Mg)$ ratio of 0.64 (Grew et al., in preparation)

A possible source of Y and heavy REE (HREE) for the Y-rich garnet could have been xenotime-(Y). Had almandine been present, it would have incorporated the Y and HREE released by breakdown of xenotime-(Y), and Y-rich garnet would not have formed.

We suggest that the breakdown of the Y-rich garnet is associated with partial melting, when it dissolved incongruently in the melt to give peritectic almandine, a process resulting in deeply embayed grains of Y-rich garnet (e.g., Fig. 2a) overgrown by markedly euhedral almandine (Fig. 2b). The evidence for K-feldspar in the moats being recrystallized melt is debatable, but the presence of melts in boudin necks (Fig. 1b) is good evidence for melting in these rocks.

The tiny grains of monazite-(Ce) and xenotime-(Y) adjacent to fine-grained apatite-(CaF) (Fig. 3d, e) could have resulted from the incongruent dissolution of apatite-(CaF), which contains minor Y and Ce. The REE-phosphate grains bear some resemblance to the monazite microcrystals formed at the apatite-liquid interface during the experimental dissolution of apatite in granitic melt (Wolf & London 1995). Coarser-grained apatite-(CaF) (Fig. 3c) could be later.

The new Y-rich garnet formed on the prograde path outside the stability field of almandine and melt, most likely at $P \sim 7-8.5$ kbar and $T \sim 700-800^\circ\text{C}$ (triangle in Fig. 4), and broke down during melting at pressures close to the first appearance of almandine in this particular bulk composition at $P \sim 8.5-9.5$ kbar and $T \sim 800-850^\circ\text{C}$.

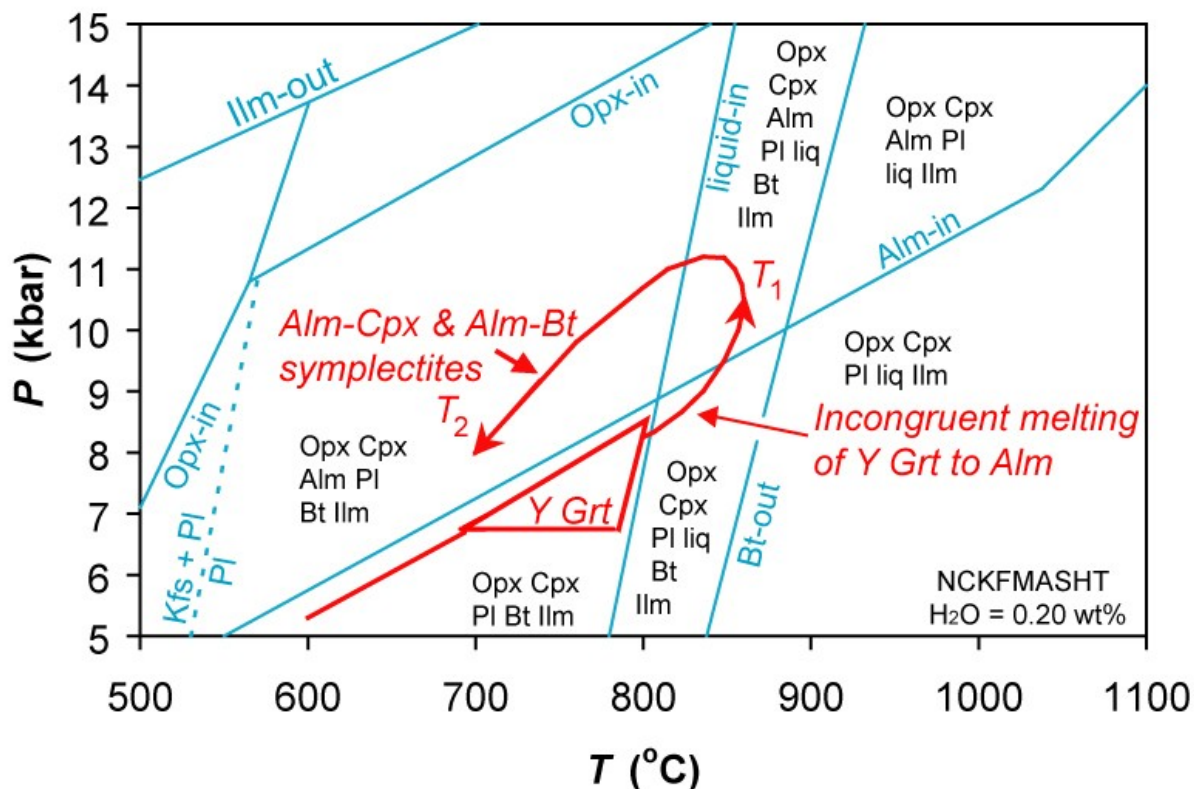


Fig. 4. P - T diagram simplified from a pseudosection calculated from the bulk composition (blue and black, Grew et al., in preparation; Marsh et al. in preparation). The path (red) is constrained by Opx-Alm-PI and Alm-Cpx assemblages and antiperthite integration for the peak conditions of 831-862 °C, 10 kbar; Alm + Hbl + Pl assemblage at T_1 ($T \sim 815$ -830 °C, $P \sim 10$ -11.5 kbar); Alm-Cpx and Alm-Bt Fe-Mg exchange in symplectites at T_2 (700 °C); and $P \sim 8$ kbar at T_2 from Culshaw et al. (1997)

Acknowledgements

JHM received support from a University of Maine Doctoral Research Fellowship. The research was supported by U.S. National Science Foundation grant OPP-0228842 to U Maine.

References

- Culshaw, N.G., Jamieson, R.A., Ketchum, J.W.F., Wodicka, N., Corrigan, D., and Reynolds, P.H., 1997, Transect across the northwestern Grenville orogen, Georgian Bay, Ontario: Polystage convergence and extension in the lower crust. *Tectonics*, 16, 966-982.
- Davidson, A., Culshaw, N.G., and Nadeau, L., 1982, A tectono-metamorphic framework for part of the Grenville Province, Parry Sound region, Ontario. Geological Survey of Canada, Paper 82-1A, 175-190.
- Enami, M., Cong, B., Yoshida, T., and Kawabe, I., 1995, A mechanism for Na incorporation in garnet: An example from garnet in orthogneiss from the Su-Lu terrane, eastern China. *American Mineralogist*, 80, 475-482.
- Kasowski, M.A. and Hogarth, D.D., 1968, Yttrian andradite from the Gatineau Park, Quebec. *The Canadian Mineralogist*, 9, 552-558.
- Wolf, M.B. and London, D., 1995, Incongruent dissolution of REE- and Sr-rich apatite in peraluminous granitic liquids: Differential apatite, monazite, and xenotime solubilities during anatexis. *American Mineralogist*, 80, 765-775.